

Unified Multi-Dataset Training for TBPS

Nilanjana Chatterjee^{†,1}, Sidhartha Garg^{†,1}, A V Subramanyam¹ and Brejesh Lall²

¹IIIT Delhi, ²IIT Delhi

nilanjanac@iiitd.ac.in, sidhartha22499@iiitd.ac.in, subramanyam@iiitd.ac.in, brejesh@ee.iitd.ac.in

Abstract

Text-Based Person Search (TBPS) has seen significant progress with vision–language models (VLMs), yet it remains constrained by limited training data and the fact that VLMs are not inherently pre-trained for pedestrian-centric recognition. Existing TBPS methods therefore rely on dataset-centric fine-tuning to handle distribution shift, resulting in multiple independently trained models for different datasets. While synthetic data can increase the scale needed to fine-tune VLMs, it does not eliminate dataset-specific adaptation. This motivates a fundamental question: can we train a single unified TBPS model across multiple datasets? We show that naive joint training over all datasets remains sub-optimal because current training paradigms do not scale to a large number of unique person identities and are vulnerable to noisy image–text pairs. To address these challenges, we propose Scale-TBPS with two contributions: (i) a noise-aware unified dataset curation strategy that cohesively merges diverse TBPS datasets; and (ii) a scalable discriminative identity learning framework that remains effective under a large number of unique identities. Extensive experiments on CUHK-PEDES, ICFG-PEDES, RSTPReid, IIITD-20K, and UFine6926 demonstrate that a single Scale-TBPS model outperforms dataset-centric optimized models and naive joint training. Code is available.

1 Introduction

Text-based Person Search (TBPS) has emerged as a critical task in computer vision, bridging the gap between natural language understanding and fine-grained visual retrieval to locate specific individuals in unconstrained image galleries. Since its formal introduction by [Li *et al.*, 2017] alongside the benchmark CUHK-PEDES dataset, the field has expanded through numerous benchmarks in recent years including ICFG-PEDES [Ding *et al.*, 2021], RSTPReid [Zhu *et al.*, 2021], IIITD-20K [Subramanyam *et al.*, 2023], and

[†] denotes equal contribution

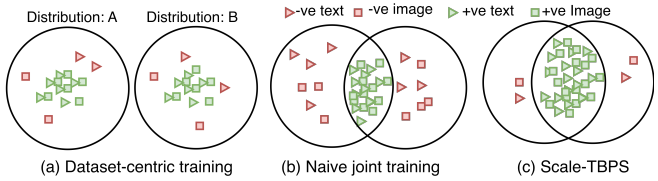


Figure 1: Illustration of Scale-TBPS. (a) illustrates the conventional dataset-centric training paradigm, where separate models are independently trained for different distributions, resulting in isolated models. (b) depicts naive joint training, where a single model is trained on merged datasets; however the learned representation fails to adequately accommodate samples from all distributions. (c) presents our proposed method, in which a single unified model is trained cohesively across distributions, effectively capturing shared semantics

UFine6926 [Zuo *et al.*, 2024]. The inception of Vision-Language Models (VLMs) such as CLIP [Radford *et al.*, 2021] and ALBEF [Li *et al.*, 2021] has yielded significant performance gains. However, these models are primarily trained on broad online corpora [Changpinyo *et al.*, 2021; Thomee *et al.*, 2016]. Though they show notable zero shot results in multiple domains, the performance in zero shot fine-grained domains still remains unsatisfactory [Wang *et al.*, 2025]. To tackle this issue, various TBPS [Qin *et al.*, 2024; Li *et al.*, 2021; Cao *et al.*, 2024; Jiang, 2023] resort to dataset level fine-tuning and propose several loss formulations and local feature networks to improve fine-grained feature extraction. Despite these advancements, the current paradigm remains heavily dataset-centric. Fine-tuning models on isolated benchmarks leads to poor cross-dataset generalization, as these models fail to account for the diverse distribution shifts caused by varying geographical locations, lighting conditions, and environmental contexts. This highlights the need for a unified approach to scale models across different shifts to maintain one unified model for all shifts.

While recent literature has explored the necessity of unified training in other vision tasks [Ci *et al.*, 2023], dedicated effort towards scaling in TBPS requires deeper investigation. In Figure 1, we show an illustrative example of how dataset-oriented models remain limited to their own specific distributions. Even when naive joint training brings these distributions into a common space, it yields subopti-

mal scaling performance for TBPS, despite having access to more training data. This occurs because the distribution shift originating from multiple benchmarks and the large number of unique person IDs are not explicitly modeled in standard TBPS paradigms. Some recent works [Yang *et al.*, 2023a; Tan *et al.*, 2024] explore person-specific pretraining from scratch; however, they still require dataset-specific fine-tuning to achieve competitive performance. Moreover, individual TBPS datasets are relatively small compared to the large-scale data typically required for training vision-language models. A model trained on unified and curated data from multiple sources can leverage greater data diversity and scale, thereby achieving superior retrieval performance.

In this work, we explore the challenges of joint training and design Scale-TBPS with two core components: a dataset curation framework to create a cohesive, noise-filtered unified dataset, and a training strategy to address the large scale of unique IDs that arises out of the unification of datasets. While conventional TBPS training paradigms are not well-suited to scale across large and diverse datasets, our approach is specifically designed to accommodate the merging of multiple distribution shifts in a scalable manner. Our contributions are as follows.

Noise-Aware Unified Dataset Curation (NDC). We first study joint training and find that naively combining multiple datasets disregards noise and results in a model that does not leverage the large scale of the data. RDE [Qin *et al.*, 2024] highlights caption noise in TBPS datasets but its iterative filtration process is not optimal for training with large-scale data. Similarly another noise filtration work, WORA-TBPS [Sun *et al.*, 2025] use unaligned models for evaluating the samples.

A recent work advocates combining multiple signals or metrics to improve bias or limitations [Wu *et al.*, 2025]. Therefore, our proposed NDC considers a set of diverse expert models trained on varied TBPS distributions. We find that some true positive pairs are far apart to be recognized, even by optimized TBPS models. Therefore, NDC relies on relative similarity ranking between text-image pairs rather than adopting a hard threshold. Combining consensus from diverse expert models enables more cohesive curation of the unified dataset. Our method is a one-time preprocessing step, making it effective for large-scale data.

Discriminative ID Learning (DIL). We introduce a training objective specifically to stabilize identity learning across diverse distribution shifts, ensuring discriminative feature embeddings. Existing TBPS methods incorporate identity-discriminative losses; however, under joint training across multiple datasets, we observe that such dataset-centric approaches consistently underperform their individually trained counterparts, despite being trained on a larger data pool. This indicates that conventional classifier-based losses struggle when the number of identities grows substantially; this phenomenon is also observed in large-scale classification settings such as face recognition [Sun *et al.*, 2014]. In the face recognition domain, angular margin-based losses have demonstrated strong discriminative capability [Deng *et al.*, 2019].

However, these formulations are primarily designed for unimodal vision tasks and are not directly applicable to text-based person search. To this end, we design a Multimodal Angular Identity loss for TBPS, which performs well with more data, overcoming the bottleneck of ID explosion of standard TBPS methods. As illustrated in Figure 1, our method brings more scalability.

2 Related Works

Text-based Person Search. TBPS aims to identify the best-matched person image given a textual description and can be regarded as a fine-grained subtask of text-based image retrieval. Owing to its practical relevance and fine-grained nature, TBPS has attracted sustained research interest. Early works primarily relied on unimodal or weakly aligned frameworks, where bridging the modality gap between visual and textual representations received a great interest [Chen *et al.*, 2022; Shao *et al.*, 2022].

With the advent of large-scale VLMs, TBPS methods have significantly benefited from improved cross-modal alignment. In particular, CLIP has become a popular choice in TBPS due to its lightweight architecture and strong transferability, and has been widely adapted for this task [Jiang, 2023; Yan *et al.*, 2023; Radford *et al.*, 2021; Cao *et al.*, 2024; Qin *et al.*, 2024]. ALBEF, although computationally heavier, provides stronger alignment capabilities and has been adopted in methods such as RaSa [Bai *et al.*, 2023].

More recently, another research direction has emerged that focuses on TBPS-specific pre-trained backbones [Yang *et al.*, 2023b; Tan *et al.*, 2024], where large multimodal language models (MLLMs) are used to generate dataset-level captions for pre-training. While these approaches improve representation learning, they still exhibit limited zero-shot performance and require subsequent dataset-specific fine-tuning to achieve competitive results. Consequently, even after TBPS-specific pre-training, the reliance on individual dataset-specific models persists. This observation motivates the need to investigate whether TBPS can be scaled towards a single unified model that can handle diverse distribution shifts.

Unified Paradigm. Although VLMs demonstrate promising zero-shot capabilities, fine-grained tasks such as TBPS and vision-based person re-identification still require task-specific fine-tuning to achieve reliable performance. Recent research trends increasingly explore unified paradigms that aim to support multiple in-domain distribution shifts within a single model. For example, ATReID [Li *et al.*, 2025] addresses illumination variations by enabling person identification across different times of day, while UniHCP [Ci *et al.*, 2023] trains a unified model for multiple human-centric perception tasks. Incremental learning has also been explored as a strategy to continually update models without catastrophic forgetting [Liu *et al.*, 2020; Kim *et al.*, 2025].

TBPS datasets exhibit substantial variation and it is impractical to assume a fixed, closed-world dataset. As new data continuously emerge due to environmental and domain variations, TBPS naturally calls for scalable and unified training strategies. In this work, we propose a dataset curation strategy that enables unified training and a discriminative ID learning

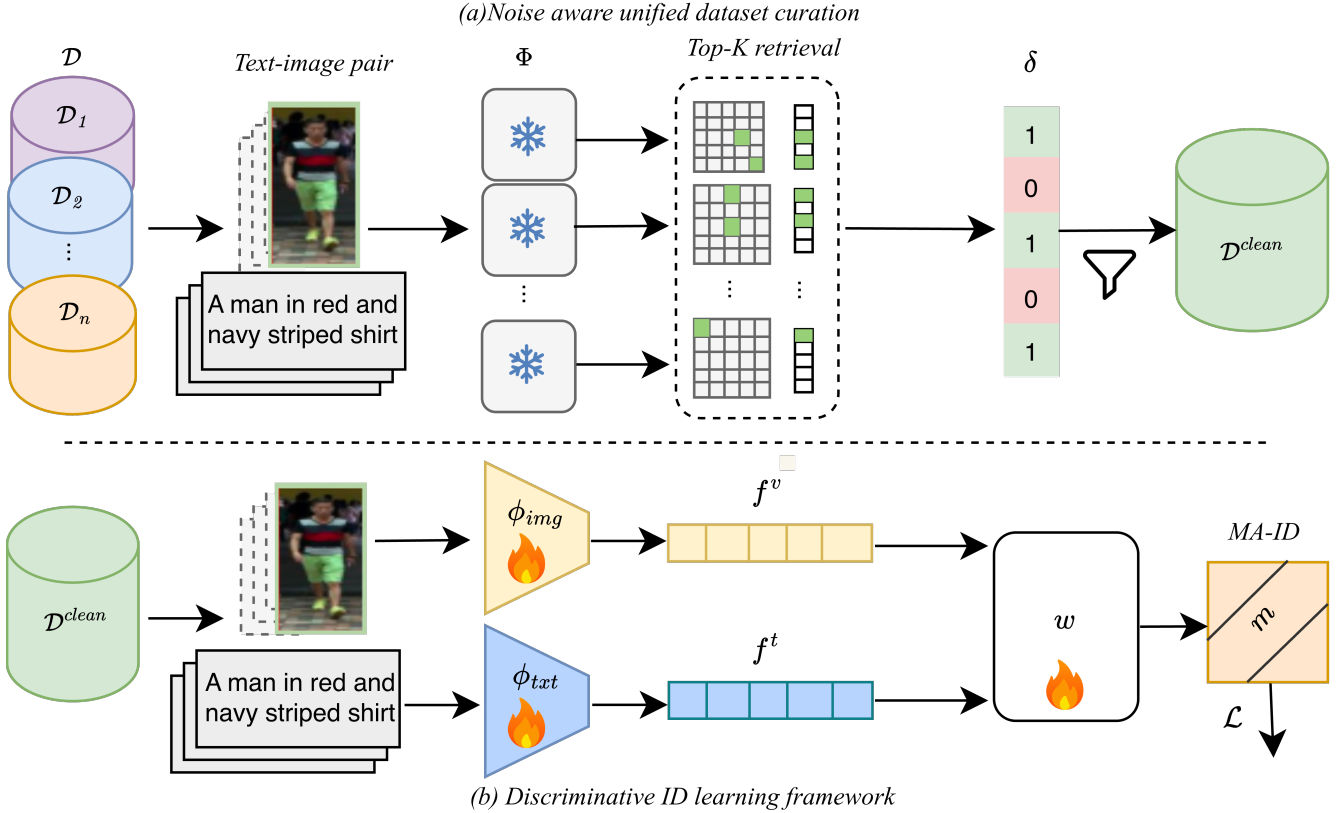


Figure 2: Overview of the proposed Scale-TBPS. (a) Noise-Aware Data Curation (NDC): Text–image pairs from the joint dataset (\mathcal{D}) are encoded using a set of pretrained and frozen models Φ . top- K retrieved samples are computed independently for each model. A pair is retained as a clean sample if it is ranked within the top- K results by at least one pretrained model; such selected pairs are highlighted in green. (b) Discriminative Identity Learning (DIL): Filtered text–image pairs from $\mathcal{D}^{\text{clean}}$ are encoded by the learnable image and text encoders and encoded features f^v and f^t are passed through a shared multimodal class weight w . MA-ID denotes the proposed multimodal angular identity loss while m denotes the margin

framework to handle a large number of unique identities.

3 Methodology

Scale-TBPS aims to learn a single unified model that can handle data scaling across all available TBPS datasets. Our method explicitly targets the cohesive merging of different data distributions while handling large volumes of unique person identities. We formulate our problem in Section 3.1, followed by our noise-aware unified dataset curation strategy (NDC) in Section 3.2. Section 3.3 explains our Discriminative Identity Learning framework (DIL) designed to scale effectively with the number of person identities.

3.1 Problem Formulation

Let there be n train-sets $\{\mathcal{D}_1, \mathcal{D}_2, \dots, \mathcal{D}_n\}$, each containing image–text pairs annotated with person identities. These datasets are merged to form a joint dataset:

$$\mathcal{D} = \bigcup_{j=1}^n \mathcal{D}_j = \{I_i, T_i, y_i\}_{i=1}^N, \quad (1)$$

where I_i and T_i denote the i -th pedestrian image and its corresponding textual description, respectively, and y_i represents a

unique person identity across the unified dataset. We employ image encoder ϕ_{img} and text encoder ϕ_{txt} initialized with CLIP weights. These encoders are jointly optimized during training to produce aligned global visual and textual representations.

Baseline. We adopt established dataset-centric TBPS model architectures as our representative baselines. To enable scalability, we design a training pipeline that can be applied on top of VLM baseline models, without modifying their core architectures.

Feature Extraction. For each image I_i , we extract a global visual representation f_i^v using an image encoder, where f_i^v corresponds to the [CLS] token or an equivalent global pooled feature. Similarly, for each text description T_i , a global textual representation f_i^t is obtained from a text encoder, using the [EOS] token.

3.2 Noise-Aware Unified Dataset Curation (NDC)

Due to annotation noise and cross-dataset distribution shifts, not all image–text pairs exhibit reliable semantic correspondence. Learning alignment confidence directly from untrained models is unreliable. Therefore, we adopt a noise-aware filtering strategy using a set of pretrained TBPS mod-

els. We perform the filtering only once and use the filtered dataset for training.

We consider a set of p pretrained person-specific models $\Phi = \{\phi_1, \phi_2, \dots, \phi_p\}$, where $p < n$. This design enables the use of diverse pretrained experts while maintaining scalability, since additional datasets can be incorporated even when the corresponding pretrained TBPS models are unavailable. The image and text encoders of ϕ_l are frozen. The ensemble thus provides robust supervision for filtering unreliable text-image pairs.

Given \mathcal{D} and ϕ_l , for every text query T_i , we examine whether its corresponding image I_i appears within the top- K retrieved images. Specifically, a text-to-image similarity matrix is computed over \mathcal{D} . The matrix is constructed using cosine similarity between ℓ_2 -normalized global text and image feature embeddings, f_i^t and f_i^v , respectively. For T_i , similarity is computed against all images in \mathcal{D} :

$$S_i = [S(f_i^t, f_1^v), S(f_i^t, f_2^v), \dots, S(f_i^t, f_N^v)], \quad (2)$$

where $S(\cdot, \cdot)$ denotes cosine similarity.

The similarity scores S_i are sorted in descending order, inducing a ranking over all images. The retrieval rank for model ϕ_l , denoted as $\text{rank}_{\phi_l}(T_i, I_i)$, is defined as the position of the ground-truth image I_i in this sorted list.

We define an indicator variable $\delta_i \in \{0, 1\}$ to determine whether a pair (T_i, I_i) is valid under the ensemble of pretrained models. A pair is considered valid if at least one pretrained model ranks the corresponding image within its top- K retrieval results:

$$\delta_i = \begin{cases} 1, & \text{if } \exists l \in \{1, \dots, p\} \text{ such that } \text{rank}_{\phi_l}(T_i, I_i) \leq K, \\ 0, & \text{otherwise.} \end{cases} \quad (3)$$

Based on this criterion, we construct a curated noise-aware dataset

$$\mathcal{D}^{\text{clean}} = \{(T_i, I_i) \in \mathcal{D} \mid \delta_i = 1\}. \quad (4)$$

which is subsequently used for training the unified model.

3.3 Discriminative ID Learning framework (DIL)

Prior methods introduce identity-specific supervision to enhance discriminative learning. While effective on individual datasets, such formulations do not scale well under unified training, where the number of identities grows significantly. The rapid expansion of the identity space leads to weak class separation with conventional classification objectives.

To address this, we design a more discriminative and scalable identity loss that enforces angular separation in a shared embedding space, enabling unified training under large-scale identity supervision. Let the feature vectors f^v and f^t be obtained by the learnable image encoder ϕ_{img} and text encoder ϕ_{txt} , respectively.

To enhance inter-class separability and scale the number of unique identities, we introduce our Multimodal Angular Identity loss. We aim to increase the distance between unique IDs by an additive angular margin m .

Let $w_j \in \mathbb{R}^d$ denote the ℓ_2 -normalized classification weight vector corresponding to the j -th identity class, where $j \in \{1, \dots, C\}$ and C is the total number of classes. For a

given sample i , we define $\theta_{i,j}$ as the angle between f_i^v and w_j , given by

$$\cos \theta_{i,j} = f_i^v \cdot w_j. \quad (5)$$

For the ground-truth class y_i , the corresponding angle is denoted as θ_{i,y_i} , which measures the angular similarity between the visual feature f_i^v and its true class weight w_{y_i} .

The margin-adjusted similarity for the target class is defined as

$$\gamma_{i,y_i} = \cos(\theta_{i,y_i} + m). \quad (6)$$

To ensure monotonicity of the angular function and maintain numerical stability, the margin-adjusted similarity is defined in a piecewise manner as

$$\gamma_{i,y_i} = \begin{cases} \cos(\theta_{i,y_i} + m), & \theta_{i,y_i} \leq \pi - m, \\ \cos(\theta_{i,y_i}) - m \sin(\pi - m), & \text{otherwise.} \end{cases} \quad (7)$$

The final logits used for training are defined as

$$z_{i,j}^v = \begin{cases} s\gamma_{i,y_i}, & j = y_i, \\ s\gamma_{i,j}, & j \neq y_i, \end{cases} \quad (8)$$

where s is a scaling factor that controls the magnitude of the logits.

The logits are then optimized using the standard cross-entropy loss:

$$\mathcal{L}_{img} = -\frac{1}{N} \sum_{i=1}^N \log \frac{\exp(z_{i,y_i}^v)}{\sum_{j=1}^C \exp(z_{i,j}^v)}. \quad (9)$$

Similarly, text-based identity loss is computed using the textual embeddings f^t and using the shared class weight w :

$$\mathcal{L}_{txt} = -\frac{1}{N} \sum_{i=1}^N \log \frac{\exp(z_{i,y_i}^t)}{\sum_{j=1}^C \exp(z_{i,j}^t)}. \quad (10)$$

Multimodal Angular Identity Loss. The final identity supervision jointly optimizes both modalities,

$$\mathcal{L}_{\text{MA-ID}} = \frac{1}{2} (\mathcal{L}_{img} + \mathcal{L}_{txt}). \quad (11)$$

This formulation enforces consistent angular discrimination across modalities, yielding compact intra-class clusters and well-separated inter-class boundaries, which is crucial for scalable unified TBPS training.

3.4 Overall training objective

We train the model using noise-aware curated dataset $\mathcal{D}^{\text{clean}}$. We adopt ranking loss TAL [Qin *et al.*, 2024]. Our model (ϕ_{img} and ϕ_{txt}) is optimized using the following overall objective,

$$\mathcal{L} = \mathcal{L}_{\text{MA-ID}} + \mathcal{L}_{TAL}. \quad (12)$$

Methods	Venue	CUHK-PEDES				ICFG-PEDES				RSTPReid			
		R-1	R-5	R-10	mAP	R-1	R-5	R-10	mAP	R-1	R-5	R-10	mAP
<i>CLIP based</i>													
CFine [Yan <i>et al.</i> , 2023]	TIP	69.57	85.93	91.15	-	60.83	76.55	82.42	-	50.55	72.50	81.60	-
CLIP [Radford <i>et al.</i> , 2021]	PMLR	68.55	86.32	91.85	61.25	56.80	75.99	82.31	31.93	56.00	80.85	87.90	44.06
IRRA [Jiang, 2023]	CVPR	73.38	89.93	93.71	66.13	63.46	80.25	85.82	38.06	60.20	81.30	88.20	47.17
TBPS-CLIP [Cao <i>et al.</i> , 2024]	AAAI	73.54	88.19	92.35	65.38	65.05	80.34	85.47	39.83	62.10	81.90	87.75	48.00
CFAM [Zuo <i>et al.</i> , 2024]	CVPR	75.60	90.53	94.36	67.27	65.38	81.17	86.35	39.42	62.45	83.55	91.10	49.50
ICL [Qin <i>et al.</i> , 2025]	CVPR	76.41	90.48	94.33	68.04	68.11	82.59	87.52	40.81	67.70	86.05	91.75	52.62
<i>Non-CLIP based</i>													
APTM [Yang <i>et al.</i> , 2023a]	MM	76.53	90.04	94.15	66.91	68.51	82.99	87.56	41.22	67.50	85.70	91.45	52.56
RaSa [Bai <i>et al.</i> , 2023]	IJCAI	76.51	90.29	94.25	69.38	65.28	80.40	85.12	41.29	66.90	86.50	91.35	52.31
WoRA-TBPS [Sun <i>et al.</i> , 2025]	MM	76.38	89.72	93.49	67.22	68.35	83.10	87.53	42.60	66.85	86.45	91.10	52.49
RDE [Qin <i>et al.</i> , 2024]	CVPR	75.94	90.14	94.12	67.56	67.68	82.47	87.36	40.06	65.35	83.95	89.90	50.88
RDE*	-	76.32	90.95	94.43	68.13	66.73	82.87	87.63	39.42	65.30	85.90	90.90	51.63
Scale-TBPS	Ours	76.85	90.22	94.23	70.05	68.22	82.09	86.80	45.16	68.90	87.00	91.65	56.00
Scale-TBPS*	Ours	77.91	91.07	94.49	70.88	68.24	83.00	87.63	45.68	71.70	87.40	91.95	58.38

Table 1: Comparison study of Scale-TBPS with existing methods. “*” denotes the results with NNN

3.5 Test time Nearest-Neighbor-Normalization (NNN)

We observe that a single text query may exhibit high similarity with multiple gallery images, resulting in biased retrieval scores. Motivated by this insight and inspired by Nearest Neighbor Normalization (NNN [Chowdhury *et al.*, 2024]), we apply similarity normalization after computing text-to-image similarities at test time. This lightweight post-processing strategy leads to a substantial improvement in retrieval performance without additional training.

Formally, the similarity between a query text T and a reference image I is defined as $S(T, I) = f^t \cdot f^v$. For each retrieval candidate I , we define a bias term $b(I)$ as a scaled average similarity between I and its top- k nearest query texts. We denote the set of \mathcal{K} queries from the reference query dataset \mathcal{D}_{test} that achieve the highest similarity scores with I . The bias term is then computed as

$$b(I) = \alpha \frac{1}{\mathcal{K}} \sum_{f_j^t \in \mathcal{D}_{top-\mathcal{K}}(I)} f_j^t \cdot f^v, \quad (13)$$

where $\mathcal{D}_{top-\mathcal{K}}(I)$ denotes the set of top- \mathcal{K} similar text candidates, retrieved from \mathcal{D}_{test} with respect to the image I .

The normalized retrieval score is obtained by subtracting the estimated bias from the original similarity, $S_N(T, I) = S(T, I) - b(I)$. In our experiments, we use both normalized and unnormalized similarity scores for computation of Rank- k and mAP. Intuitively, NNN exploits the nearest \mathcal{K} query embeddings to mitigate hubness and better differentiate visually similar retrieval candidates. When integrated with retrieval systems, this procedure introduces only sublinear overhead and adds a constant-factor cost to retrieval runtime.

4 Experiments

In this section, we conduct extensive experiments to comprehensively evaluate the effectiveness and scalability of the proposed Scale-TBPS framework.

4.1 Experimental Details

For our unified dataset curation, we combine training set of four widely used text-based person search benchmarks:

CUHK-PEDES [Li *et al.*, 2017], ICFG-PEDES [Ding *et al.*, 2021], RSTPReid [Zhu *et al.*, 2021] and IIITD-20K [Subramanyam *et al.*, 2023]. We utilize three pretrained models trained individually on CUHK-PEDES, ICFG-PEDES, and RSTPReid to filter pairs. Notably, we intentionally exclude models trained on IIITD-20K in order to explicitly evaluate the scalability of our framework. Our unified dataset contains a total of 30,957 unique identities in the training set, compared to 11,003, 3,102, 3,701, 15000 training set identities in CUHK-PEDES, ICFG-PEDES, RSTPReid and IIITD-20K, respectively.

We set $K=25$. Following [Chowdhury *et al.*, 2024], we use $\alpha = 0.75$ and $\mathcal{K} = 16$, and do not tune them for any of the experiments. We employ a discriminative identity classifier with a fixed scale of $s = 30$ and an angular margin of $m = 0.35$. We use RDE as our baseline. We follow the training configurations of RDE. We follow the standard test protocols used across all TBPS datasets. We evaluate retrieval performance using Rank- k accuracy at $k = \{1, 5, 10\}$, and mean Average Precision (mAP).

4.2 Main results

As shown in Table 1, we compare Scale-TBPS with state-of-the-art dataset-centric methods, where each model is trained independently on a single dataset. In contrast, Scale-TBPS learns a single unified model and outperforms these dataset-specific approaches in most of the metrics. We report results for Scale-TBPS with and without test-time similarity normalization NNN, where Scale-TBPS* denotes the variant using normalization. Scale-TBPS uses CLIP as the backbone, but we report discussion with both CLIP-based and non-CLIP-based approaches.

Comparison against CLIP-based methods. Scale-TBPS consistently outperforms RDE across datasets and metrics. In particular, we see a significant gain in terms of mAP. We see a gain of approximately 5.1% in mAP on both ICFG-PEDES and RSTPReid. In the transductive setting where test time normalization is applied, compared to RDE*, Scale-TBPS* shows a 2.75%, 6.26%, and 6.75% increase in mAP on CUHK-PEDES, ICFG-PEDES, and RSTPReid, respectively. On RSTPReid, our method shows a 6.40% improve-

Method	R-1	R-5	R-10	mAP
CLIP	73.48	91.82	95.60	81.69
IRRA [Jiang, 2023]	77.08	—	—	—
RDE [Qin <i>et al.</i> , 2024]	80.90	94.48	97.02	87.04
Scale-TBPS (Ours)	82.42	95.50	97.42	88.28
Scale-TBPS* (Ours)	85.20	96.56	98.04	90.31

Table 2: Comparison results on IIITD-20K

ment in Rank-1 accuracy compared to RDE*.

The CLIP-based state-of-the-art method ICL [Qin *et al.*, 2025] relies on multimodal large language models (MLLMs) [Wang *et al.*, 2024] for data augmentation. Despite not employing such auxiliary components, Scale-TBPS surpasses ICL in both Rank-1 and mAP. Overall, our single unified model outperforms all CLIP-based methods across metrics.

To study the effect of NNN, we also report RDE*. We use the values of α and K as suggested in [Chowdhury *et al.*, 2024] and do not tune them either for Scale-TBPS or RDE. RDE* shows only a nominal gain of 0.38% in Rank-1 on CUHK-PEDES over RDE, whereas Scale-TBPS* shows a 1.15% boost on the same metric compared to Scale-TBPS. Further, Rank-1 accuracy decreases for ICFG-PEDES and RSTPReid. While NNN effectively mitigates candidate bias $b(I)$ for Scale-TBPS, its benefit is less pronounced for RDE, where dataset-centric training calibrates similarity scores and reduces hubness.

Comparison against non-CLIP-based methods. Scale-TBPS outperforms RaSa [Bai *et al.*, 2023], which is ALBEF-based, even though ALBEF is generally considered a stronger backbone than CLIP. On ICFG-PEDES it shows a 2.94% gain in Rank-1, while on RSTPReid it shows a 2% gain. We also compare against APTM and WoRA-TBPS, whose backbones are pre-trained on pedestrian-specific data and thus exhibit strong capabilities. Notably, CLIP-based methods are significantly lighter in terms of parameter count. Compared to APTM [Yang *et al.*, 2023b] and WoRA-TBPS, our method outperforms APTM on both CUHK-PEDES and RSTPReid. In contrast, the baseline RDE fails to surpass APTM and RaSa, whereas our method achieves consistent improvements over both. These results demonstrate that properly designed unified model can outperform different dataset-centric models. Our CLIP based method gives competing performance against stronger backbones too.

Results on IIITD-20K. We do not use IIITD-20K trained model to filter data. We deliberately exclude model trained on IIITD-20K to explicitly evaluate scalability of our framework. We find that our method with and without test time normalization outperforms the baseline RDE by a significant margin. We observe 1.52% increase in Rank-1 accuracy in Scale-TBPS and an additional 2.78% accuracy increase are observed with Scale-TBPS* as reported in Table 2. Thus the substantial increase validates the scalability of our method.

Results on UFine6926. As UFine6926 [Zuo *et al.*, 2024] is not included in our training paradigm, we evaluate our model in a zero-shot setting on this dataset, as reported in Table 3. For comparison, we report results from prior methods that are trained exclusively on CUHK-PEDES, as this

Method	R-1	R-5	R-10	mAP
IRRA [Jiang, 2023]	37.51	54.92	64.29	40.76
RDE [Qin <i>et al.</i> , 2024]	40.37	57.49	66.05	42.68
ICL [Qin <i>et al.</i> , 2025]	46.40	63.55	72.08	48.68
Scale-TBPS (Ours)	44.87	63.57	72.13	46.74
Scale-TBPS* (Ours)	54.10	71.76	79.26	56.00

Table 3: Zero-shot Performance Comparison on UFine6926

Method	CUHK-PEDES		ICFG-PEDES		RSTPReid	
	R-1	mAP	R-1	mAP	R-1	mAP
Naive-IRRA	73.26	66.70	62.34	38.98	65.05	53.22
Naive-RDE	76.40	68.32	66.03	40.68	67.00	54.14
NDC	75.97	68.02	66.42	40.92	70.15	54.75
DIL	76.09	68.96	66.60	42.81	66.60	54.30
NDC+DIL	76.85	70.05	68.22	45.16	68.90	56.00

Table 4: Ablation study for NDC and DIL. NDC+DIL is the Scale-TBPS method

setting yields the strongest performance in their respective works. Our Scale-TBPS shows a 4.5% gain in Rank-1 and a 4.06% gain in mAP. It is observed that Scale-TBPS* provides a significant boost in zero-shot performance, notably a 9.23% gain in Rank-1 compared to Scale-TBPS. Hence, our proposed method generalizes well to unseen domain.

4.3 Ablation and Hyperparameter Study

We analyze the contribution of the two core components of Scale-TBPS in Table 4: (i) noise-aware unified data curation (NDC), and (ii) discriminative identity learning framework (DIL) for scaling to a large number of unique identities.

For fair comparison, we include two strong naive joint training baselines, where IRRA and RDE are individually trained with the joint dataset. We keep RDE’s original filtering protocols. As reported in Table 4, even though naive joint training leverages a larger volume of training data, it fails to yield better results across all datasets. In particular, it underperforms compared to RDE model on ICFG-PEDES. We also report the performance of our modules NDC and DIL independently.

Compared to naive joint training, NDC improves both Rank-1 and mAP on ICFG-PEDES and RSTPReid. On CUHK-PEDES, NDC shows a marginal drop. On the other hand, DIL shows significant improvement over the naive method on ICFG-PEDES. Our proposed method NDC combined with DIL outperforms naive method by 1% in CUHK-PEDES and nearly 2% in ICFG-PEDES and RSTPReid in Rank-1 accuracy. In terms of mAP, our method outperforms the naive approach by 1.73% on CUHK-PEDES, 4.48% on ICFG-PEDES, and 1.86% on RSTPReid.

Analysis of DIL. To demonstrate the effectiveness of the proposed DIL framework in separating identity classes, we visualize the learned feature distributions using t-SNE [Maaten and Hinton, 2008]. We compare our method against naive joint training. As illustrated in Figure 3, the proposed method yields well-structured clusters characterized by strong intra-class compactness and clear inter-class separability. In contrast, naive joint training produces overlapping

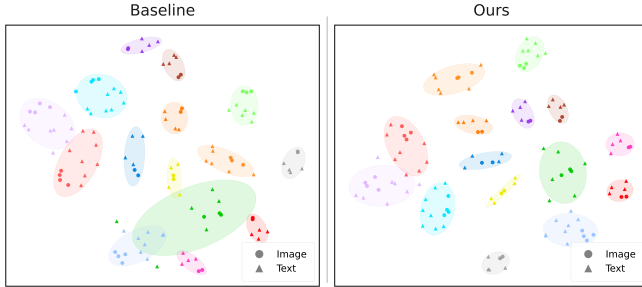


Figure 3: t-SNE visualization comparing naive joint training and the proposed DIL. Different color signifies different IDs. Our method exhibits tighter intra-class clustering and improved inter-class separation

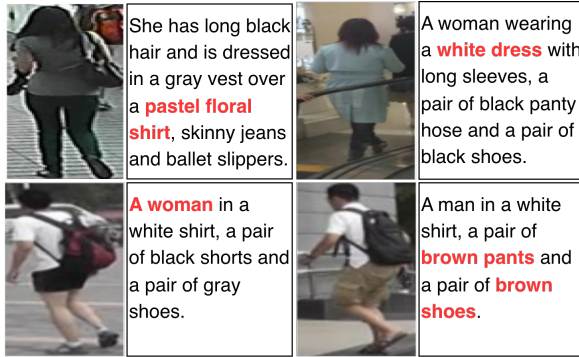


Figure 4: Examples of noisy samples removed by our NDC module. Noisy parts are highlighted in red

clusters, indicating weaker identity discrimination. These observations confirm that DIL effectively enhances discriminative feature learning under a large number of identities.

Analysis of NDC. We show qualitative examples that our NDC module filters out in Figure 4. Since pair selection is guided by three diverse TBPS models, the filtering procedure is able to remove noisy pairs while retaining a substantial portion of useful data. NDC module is a one-time preprocessing step that takes only 556.47 seconds on a single Nvidia A100 GPU to filter the entire joint dataset of 1,69,810 text-image pairs, making it easily scalable to large volumes of data.

In Figure 5 we see for $K=25$, CUHK-PEDES and ICFG-PEDES retains approximately 90% of their data. In contrast, RSTPReid retains only 60.3% of the data. This is consistent with prior work, which identifies RSTPReid as one of the noisiest TBPS benchmarks. We intentionally exclude any model trained on IIITD-20K during the filtering stage. Even under this constraint, approximately 82% of the IIITD-20K data is retained, validating that our method can effectively scale to new TBPS distributions using a limited set of pre-trained TBPS experts.

Hyperparameter Analysis. We conduct a hyperparameter sensitivity analysis on the margin (m) and scale (s) used in our DIL. m is used to set the boundary between different identity classes, and s signifies the sharpness of logits in DIL. The hyperparameters are selected based on Rank-1 accuracy on CUHK-PEDES following previous TBPS methods.

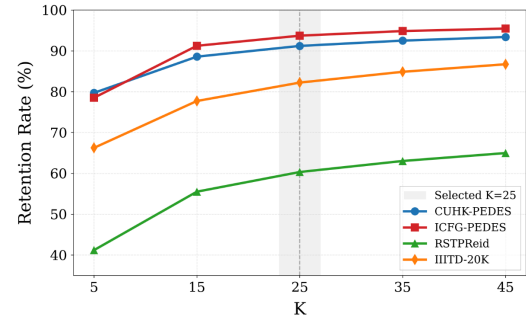


Figure 5: Data retention rates (%) after filtration by our NDC module across various values of K for different TBPS datasets.

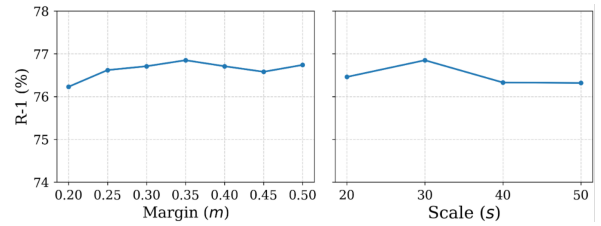


Figure 6: Hyperparameter Sensitivity Analysis on CUHK-PEDES

In Figure 6 we show that the best results are achieved with $m = 0.35$ and $s = 30$. The proposed method exhibits strong robustness to hyperparameter variations, with Rank-1 accuracy fluctuating by less than 1% across a wide range of values.

In Figure 5, we present a comprehensive study of dataset percentage retention with respect to different K values. Our NDC module selects a pair when the corresponding image is retrieved within the Top- K samples for a given caption. We observe that at $K = 25$, the retention curve plateaus, and we choose this value for our experiments, as below this point the data retention drops, while beyond it the increase is only marginal.

We provide code and additional results in the supplementary material.

5 Conclusion

In this work, we propose Scale-TBPS, a unified training paradigm that enables learning a single model across multiple text-based person search datasets. We introduce a noise-aware data curation strategy to cohesively merge multiple datasets, along with a discriminative ID learning framework designed to effectively handle the rapid growth in unique identities that arises with dataset merging. Comprehensive experiments on CUHK-PEDES, RSTPReid, ICFG-PEDES, and IIITD-20K demonstrate that a single Scale-TBPS model consistently matches or surpasses dataset-specific state-of-the-art methods, as well as naive joint training, under diverse distribution shifts. Furthermore, we demonstrate zero-shot robustness on UFine6926, highlighting strong generalization to previously unseen data. Additionally, we observe that test time normalization significantly boosts the performance of Scale-TBPS compared to other methods.

References

[Bai *et al.*, 2023] Yang Bai, Min Cao, Daming Gao, Ziqiang Cao, Chen Chen, Zhenfeng Fan, Liqiang Nie, and Min Zhang. Rasa: Relation and sensitivity aware representation learning for text-based person search. In Edith Elkind, editor, *Proceedings of the Thirty-Second International Joint Conference on Artificial Intelligence, IJCAI-23*, pages 555–563. International Joint Conferences on Artificial Intelligence Organization, 8 2023. Main Track.

[Cao *et al.*, 2024] Min Cao, Yang Bai, Ziyin Zeng, Mang Ye, and Min Zhang. An empirical study of clip for text-based person search. In *AAAI*, volume 38, pages 465–473, 2024.

[Changpinyo *et al.*, 2021] Soravit Changpinyo, Piyush Sharma, Nan Ding, and Radu Soricut. Conceptual 12m: Pushing web-scale image-text pre-training to recognize long-tail visual concepts. In *Proceedings of the IEEE/CVF conference on computer vision and pattern recognition*, pages 3558–3568, 2021.

[Chen *et al.*, 2022] Yuhao Chen, Guoqing Zhang, Yujiang Lu, Zhenxing Wang, and Yuhui Zheng. Tipcb: A simple but effective part-based convolutional baseline for text-based person search. *Neurocomputing*, 494:171–181, 2022.

[Chowdhury *et al.*, 2024] Neil Chowdhury, Franklin Wang, Sumedh Shenoy, Douwe Kiela, Sarah Schwettmann, and Tristan Thrush. Nearest neighbor normalization improves multimodal retrieval. In Yaser Al-Onaizan, Mohit Bansal, and Yun-Nung Chen, editors, *Proceedings of the 2024 Conference on Empirical Methods in Natural Language Processing*, pages 22571–22582, Miami, Florida, USA, November 2024. Association for Computational Linguistics.

[Ci *et al.*, 2023] Yuanzheng Ci, Yizhou Wang, Meilin Chen, Shixiang Tang, Lei Bai, Feng Zhu, Rui Zhao, Fengwei Yu, Donglian Qi, and Wanli Ouyang. Unihcp: A unified model for human-centric perceptions. In *Proceedings of the IEEE/CVF conference on computer vision and pattern recognition*, pages 17840–17852, 2023.

[Deng *et al.*, 2019] Jiankang Deng, Jia Guo, Nianan Xue, and Stefanos Zafeiriou. Arcface: Additive angular margin loss for deep face recognition. In *Proceedings of the IEEE/CVF conference on computer vision and pattern recognition*, pages 4690–4699, 2019.

[Ding *et al.*, 2021] Zefeng Ding, Changxing Ding, Zhiyin Shao, and Dacheng Tao. Semantically self-aligned network for text-to-image part-aware person re-identification. *arXiv preprint arXiv:2107.12666*, 2021.

[Jiang, 2023] Mang Jiang. Cross-modal implicit relation reasoning and aligning for text-to-image person retrieval. In *CVPR*, pages 2787–2797, 2023.

[Kim *et al.*, 2025] Shiwon Kim, Dongjun Hwang, Sungwon Woo, and Rita Singh. Does prior data matter? exploring joint training in the context of few-shot class-incremental learning. In *Proceedings of the IEEE/CVF International Conference on Computer Vision*, pages 5185–5194, 2025.

[Li *et al.*, 2017] Shuang Li, Tong Xiao, Hongsheng Li, Bolei Zhou, Dayu Yue, and Xiaogang Wang. Person search with natural language description. In *CVPR*, pages 1970–1979, 2017.

[Li *et al.*, 2021] Junnan Li, Ramprasaath Selvaraju, Akhilesh Gotmare, Shafiq Joty, Caiming Xiong, and Steven Chu Hong Hoi. Align before fuse: Vision and language representation learning with momentum distillation. In *NeurIPS*, volume 34, pages 9694–9705, 2021.

[Li *et al.*, 2025] Xulin Li, Yan Lu, Bin Liu, Jiaze Li, Qin-hong Yang, Tao Gong, Qi Chu, Mang Ye, and Nenghai Yu. Towards anytime retrieval: A benchmark for anytime person re-identification. In James Kwok, editor, *Proceedings of the Thirty-Fourth International Joint Conference on Artificial Intelligence, IJCAI-25*, pages 1467–1475. International Joint Conferences on Artificial Intelligence Organization, 8 2025. Main Track.

[Liu *et al.*, 2020] Yaoyao Liu, Yuting Su, An-An Liu, Bernt Schiele, and Qianru Sun. Mnemonics training: Multi-class incremental learning without forgetting. In *Proceedings of the IEEE/CVF conference on Computer Vision and Pattern Recognition*, pages 12245–12254, 2020.

[Maaten and Hinton, 2008] Laurens van der Maaten and Geoffrey Hinton. Visualizing data using t-sne. *Journal of machine learning research*, 9(Nov):2579–2605, 2008.

[Qin *et al.*, 2024] Yang Qin, Yingke Chen, Dezhong Peng, Xi Peng, Joey Tianyi Zhou, and Peng Hu. Noisy-correspondence learning for text-to-image person re-identification. In *CVPR*, pages 27197–27206, 2024.

[Qin *et al.*, 2025] Yang Qin, Chao Chen, Zhihang Fu, Dezhong Peng, Xi Peng, and Peng Hu. Human-centered interactive learning via mllms for text-to-image person re-identification. In *Proceedings of the Computer Vision and Pattern Recognition Conference*, pages 14390–14399, 2025.

[Radford *et al.*, 2021] Alec Radford, Jong Wook Kim, Chris Hallacy, Aditya Ramesh, Gabriel Goh, Sandhini Agarwal, Girish Sastry, Amanda Askell, Pamela Mishkin, Jack Clark, et al. Learning transferable visual models from natural language supervision. In *ICML*, pages 8748–8763. PMLR, 2021.

[Shao *et al.*, 2022] Zhiyin Shao, Xinyu Zhang, Meng Fang, Zhifeng Lin, Jian Wang, and Changxing Ding. Learning granularity-unified representations for text-to-image person re-identification. In *ACM MM*, pages 5566–5574, 2022.

[Subramanyam *et al.*, 2023] A Venkata Subramanyam, Vibhu Dubey, Niranjan Sundararajan, and Brejesh Lall. Dense captioning for text-image reid. In *ICVGIP*, pages 1–8, 2023.

[Sun *et al.*, 2014] Yi Sun, Yuheng Chen, Xiaogang Wang, and Xiaoou Tang. Deep learning face representation by joint identification-verification. *Advances in neural information processing systems*, 27, 2014.

[Sun *et al.*, 2025] Jintao Sun, Hao Fei, Gangyi Ding, and Zhedong Zheng. From data deluge to data curation: A filtering-wora paradigm for efficient text-based person search. In *Proceedings of the ACM on Web Conference 2025*, pages 2341–2351, 2025.

[Tan *et al.*, 2024] Wentan Tan, Changxing Ding, Jiayu Jiang, Fei Wang, Yibing Zhan, and Dapeng Tao. Harnessing the power of mllms for transferable text-to-image person reid. In *Proceedings of the IEEE/CVF Conference on Computer Vision and Pattern Recognition*, pages 17127–17137, 2024.

[Thomee *et al.*, 2016] Bart Thomee, David A Shamma, Gerald Friedland, Benjamin Elizalde, Karl Ni, Douglas Poland, Damian Borth, and Li-Jia Li. Yfcc100m: The new data in multimedia research. *Communications of the ACM*, 59(2):64–73, 2016.

[Wang *et al.*, 2024] Peng Wang, Shuai Bai, Sinan Tan, Shijie Wang, Zhihao Fan, Jinze Bai, Keqin Chen, Xuejing Liu, Jialin Wang, Wenbin Ge, et al. Qwen2-vl: Enhancing vision-language model’s perception of the world at any resolution. *arXiv preprint arXiv:2409.12191*, 2024.

[Wang *et al.*, 2025] Yue Wang, Shuai Xu, Xuelin Zhu, and Yicong Li. Msci: Addressing clip’s inherent limitations for compositional zero-shot learning. *arXiv preprint arXiv:2505.10289*, 2025.

[Wu *et al.*, 2025] Sitong Wu, Haoru Tan, Yukang Chen, Shaofeng Zhang, Jingyao Li, Bei Yu, Xiaojuan Qi, and Jiaya Jia. Mixture-of-scores: Robust image-text data valuation via three lines of code. In *Proceedings of the IEEE/CVF International Conference on Computer Vision*, pages 24603–24614, 2025.

[Yan *et al.*, 2023] Shuanglin Yan, Neng Dong, Liyan Zhang, and Jinhui Tang. Clip-driven fine-grained text-image person re-identification. *TIP*, 32:6032–6046, 2023.

[Yang *et al.*, 2023a] Shuyu Yang, Yinan Zhou, Zhedong Zheng, Yaxiong Wang, Li Zhu, and Yujiao Wu. Towards unified text-based person retrieval: A large-scale multi-attribute and language search benchmark. In *ACM MM*, pages 4492–4501, 2023.

[Yang *et al.*, 2023b] Shuyu Yang, Yinan Zhou, Zhedong Zheng, Yaxiong Wang, Li Zhu, and Yujiao Wu. Towards unified text-based person retrieval: A large-scale multi-attribute and language search benchmark. In *Proceedings of the 31st ACM international conference on multimedia*, pages 4492–4501, 2023.

[Zhu *et al.*, 2021] Aichun Zhu, Zijie Wang, Yifeng Li, Xili Wan, Jing Jin, Tian Wang, Fangqiang Hu, and Gang Hua. Dssl: Deep surroundings-person separation learning for text-based person retrieval. In *ACM MM*, pages 209–217, 2021.

[Zuo *et al.*, 2024] Jialong Zuo, Hanyu Zhou, Ying Nie, Feng Zhang, Tianyu Guo, Nong Sang, Yunhe Wang, and Changxin Gao. Ufinebench: Towards text-based person retrieval with ultra-fine granularity. In *Proceedings of the IEEE/CVF Conference on Computer Vision and Pattern Recognition*, pages 22010–22019, 2024.